Available online at www.sciencedirect.com
SCIENCE DIRECT®
Journal of Power Sources 119–121 (2003) 8–15
JOURNAL OF POWER SOURCES
www.elsevier.com/locate/jpowsour

Purification process of natural graphite as anode for Li-ion batteries: chemical versus thermal

K. Zaghib[a,*], X. Song[b], A. Guerfi[a], R. Rioux[a], K. Kinoshita[b]

[a]*Institut de Recherche, Service Chimie des Materiaux, d'Hydro-Québec (IREQ), 1800 Boul., Lionel-Boulet Varennes, Que., Canada J3X 1S1*
[b]*Environmental Energy Technologies Division, Lawrence Berkeley National Laboratory, Berkeley, CA 94720, USA*

Abstract

The intercalation of Li ions in natural graphite that was purified by chemical and thermal processes was investigated. A new chemical process was developed that involved a mixed aqueous solution containing 30% H_2SO_4 and 30% NH_xF_y heated to 90 °C. The results of this process are compared to those obtained by heating the natural graphite from 1500 to 2400 °C in an inert environment (thermal process). The first-cycle coulombic efficiency of the purified natural graphite obtained by the chemical process is 91 and 84% after the thermal process at 2400 °C. Grinding the natural graphite before or after purification had no significant effect on electrochemical performance at low currents. However, grinding to a very small particle size before purification permitted optimization of the size distribution of the particles, which gives rise to a more homogenous electrode. The impurities in the graphite play a role as microabrasion agents during grinding which enhances its hardness and improves its mechanical properties. Grinding also modifies the particle morphology from a 2- to a 3-D structure (similar in shape to a potato). This potato-shaped natural graphite shows high reversible capacity at high current densities (about 90% at 1*C* rate). Our analysis suggests that thermal processing is considerably more expensive than the chemical process to obtain purified natural graphite.

Keywords: Lithium intercalation; Natural graphite; Chemical; Purification; Thermal treatment

1. Introduction

Lithium-ion batteries are now widely used in consumer electronic devices such as cellular telephones, camcorders and portable computers. There is also a strong interest in utilizing Li-ion batteries for transportation applications. The United States Advanced Battery Consortium (USABC) was formed in the early 1990s to develop large-scale rechargeable lithium batteries for electric vehicles (EVs). This effort was followed by the formation of the Partnership for the New Generation Vehicle (PNGV), which has a goal of developing a passenger automobile that can achieve the equivalent of 80 mpg. Both the USABC and PNGV Programs supported the development of Li-ion batteries. One key requirement for Li-ion batteries in EVs is that low-cost materials are needed to reduce the cost of the battery [1].

Natural graphite (NG) is an attractive material for Li-ion batteries because of its wide availability in countries such as Brazil, Canada, China, Russia and Sweden. In addition, the particle size and shape (e.g. flake, spherical, exfoliated) of natural graphite can be modified. Its high capacity (372 mAh/g) and low working voltage yields Li-ion cells with high energy density (Wh/kg). Grinding and purification are key processing steps to obtain useful natural graphite. It is difficult to find many published papers related to this topic, but several patents are already pending or published. Superior Graphite Co. [2] produces graphitized carbon with <0.5% S by heat treatment to 2300 °C in nitrogen. Recently, Sanyo [3] used a similar process for purifying natural graphite. The results suggest that heat treatment (>2300 °C) removes impurities and improves cycle life of natural graphite in Li-ion cells. The impurities react with the electrolyte resulting in its decomposition. Unfortunately, Sanyo did not mention the type and concentration of impurities present in the graphite.

Kyushu Refract Co. [4] used a chemical treatment to purify natural graphite in aqueous mineral acid plus HF (up to 46% concentration). Kansai Coke & Chemical Co. [5] reported a purity of 99.9% after natural graphite was treated in aqueous HF (10–70% concentration). To develop improved and low-cost carbonaceous materials ($<10 kg^{-1}) for Li-ion batteries, we initiated studies to purify natural graphite by a new chemical process that does not involve using HF. Grinding the sample to very small particle sizes before purification to optimize the size distribution of the particles, facilitated the

* Corresponding author. Tel.: +1-450-652-8019; fax: +1-450-652-8424.
E-mail address: karimz@ireq.ca (K. Zaghib).

0378-7753/03/$ – see front matter
doi:10.1016/S0378-7753(03)00116-2

fabrication of homogeneous electrode structures. The impurities found in the natural graphite act as a microabrasion agent during grinding helps to modify the particle shape from a 2- to a 3-D structure, and enhance its hardness and improves its mechanical properties. The aim of this paper is to compare the Li-ion cell electrochemical performance of natural graphite, prepared by chemical and thermal processes [3]. We attempted to correlate the cycle life (capacity fade) of cells with purified natural graphite that initially contained different impurities (Si, Fe, Ca, Mo). An effort was also undertaken to identify the elements, which were not removed by purification.

2. Experimental

The concentration of impurities in natural graphite (NATIONAL DE GRAFITE LTD, Brazil) is summarized in Table 1. The as-received sample has an average particle size of 323 μm, which is air-milled to an average particle size of 20 μm. At this stage, the natural graphite has a purity of 98.5%, but still contains significant amounts of Al and Fe. The graphite (30 g) is then leached in a mixed aqueous solution containing 30% H_2SO_4 and 30% NH_xF_y (106 ml) heated at 90 °C, for 1–4 h. The solid is then filtered, washed with copious amounts of water, and dried at 120 °C for 24 h. Other samples of natural graphite from the same source were heat-treated in a Labmaster furnace (Thermal Technology Inc.) in flowing He for 2 h at a constant temperature between 1000 and 2400 °C.

X-ray diffraction (XRD) analysis (Siemens D500 Diffractometer) was used to determine the $d_{0\,0\,2}$ spacing and the crystallite size, L_c. The Brunauer–Emmet–Teller (BET) surface area was measured with a Quantachrome Autosorb automated gas sorption system using N_2 gas.

The concentration of impurities in the graphite was determined by using an inductively coupled plasma optical emission spectrometer (Perkin-Elmer, Optima 4300). Secondary electron microscopy (SEM) and energy dispersive X-ray (EDX) analysis were also used in the analysis of the impurities.

The working electrode was fabricated from a mixture of natural graphite and poly(vinylidene fluoride) (PVDF) dissolved in 1-methyl-2-pyrrolidinone (NMP). The slurry was spread onto a copper grid (Exmet Corp., Naugatuck, CT) and

Table 1
Impurity content in Brazilian graphite (NATIONAL DE GRAFITE LTD)

Chemical substance (ppm)													
Fe	Mo	Sb	As	V	Cr	Cu	Ni	Pb	Co	Ca	Al	Ge	Si
103	1.5	<1	<0.5	9.7	6.5	4.2	0.3	<1	0.5	3	528.8	<1	0.3

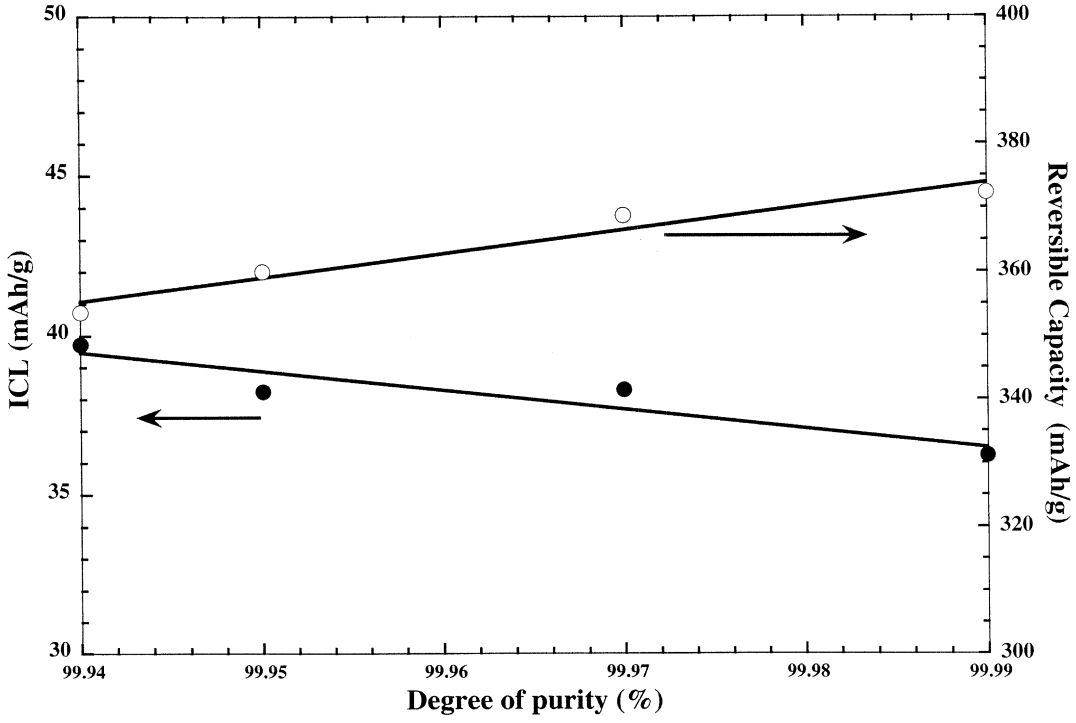

Fig. 1. Relationship between purity of natural graphite obtained by chemical process and electrochemical performance parameters (reversible capacity, ICL). Solid lines indicate trend of the data.

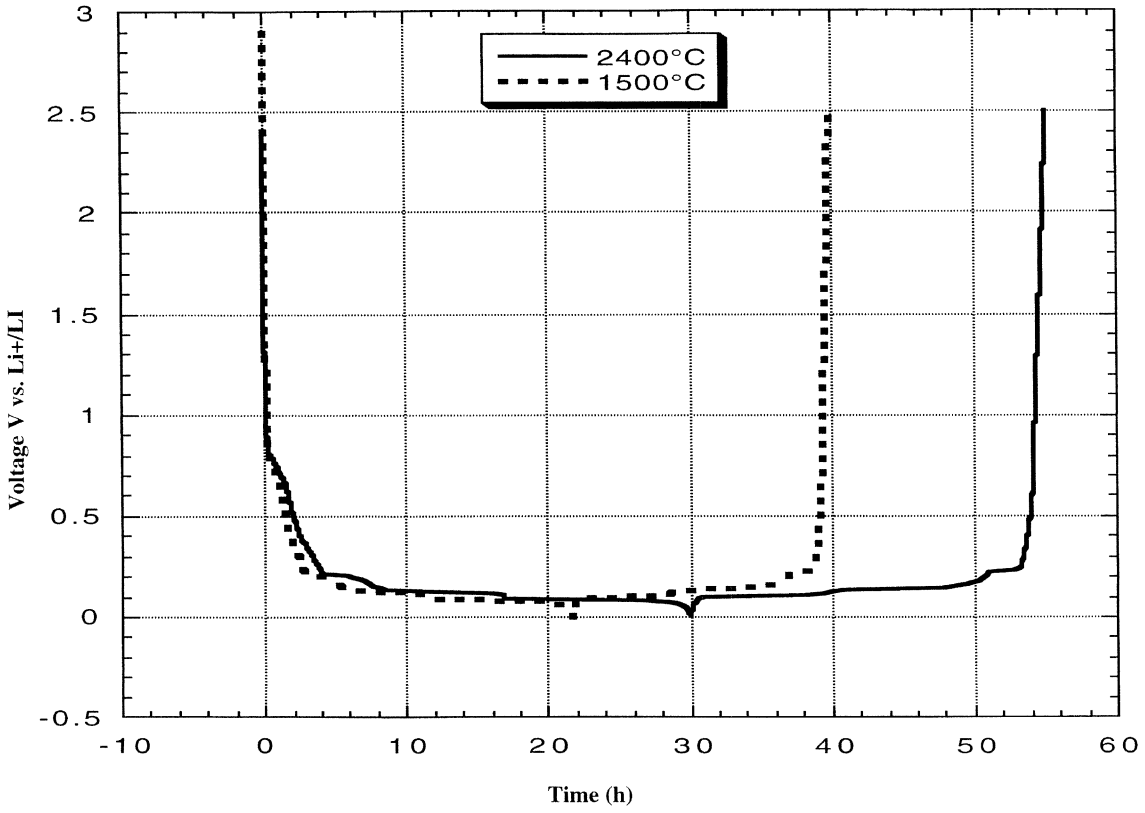

Fig. 2. Charge–discharge profiles for natural graphite heat treated at 1500 and 2400 °C at a discharge–charge rate of 15.5 mA/g (*C*/24 rate).

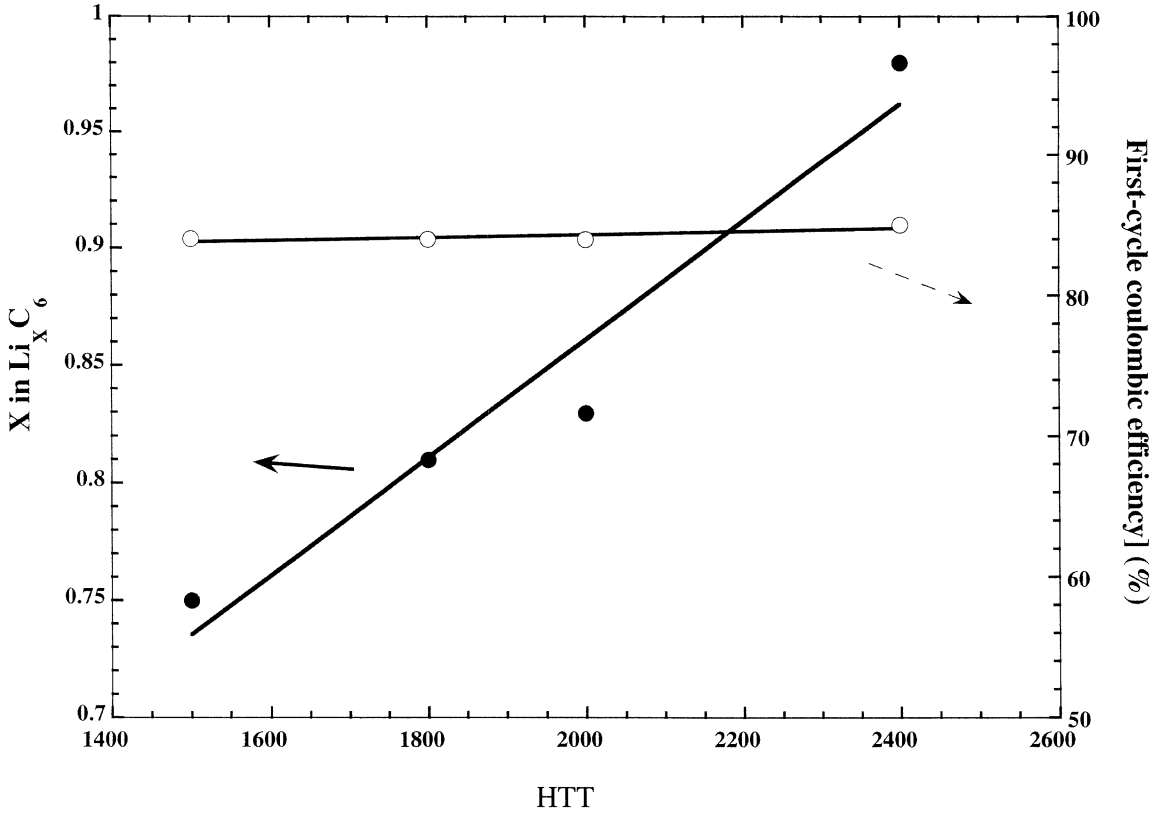

Fig. 3. Composition of intercalated graphites, x in Li_xC_6, and coulombic efficiency vs. heat-treatment temperature.

dried under vacuum at 95 °C for 24 h. A typical electrode thickness is about 200 μm, and the electrode area is 12 cm^2 (6 cm^2 per side). The working electrodes were evaluated in a three-electrode cell that contained metallic Li as both the counter and reference electrodes. The cells were built in a glove box under an Ar atmosphere containing less than 5 ppm humidity. Electrochemical measurements of the charge–discharge of graphite were conducted in an electrolyte containing 1 M $LiClO_4$ in 1:1 (volume ratio) EC–DMC (Tomiyama Pure Chemical Industries Ltd.). The cells were cycled between 2.5 and 0 V versus Li/Li^+ with a MacPile II (Bio Logic, France).

The electrochemical experiments involved the following procedure. The electrode is discharged (Li^+-ion intercalation) at *C*/24 to form a stable solid electrolyte interface (SEI) layer. A constant current is applied until the electrode potential reaches 0 mV, then the electrode is charged (Li^+ de-intercalation) at the *C*/24 rate. Following the formation cycle, the electrode is cycled at higher discharge rates up to 1*C* rate.

3. Discussion of results

Table 2 shows the concentration of impurities in NG obtained after heat treatment at 1500–2400 °C and chemical processing for 2–4 h in 30% H_2SO_4 and 30% NH_xF_y. Almost all of the samples showed a decrease in the wt.% of impurities relative to the reference (REF) sample as the heat-treatment temperature increases. A similar trend was also observed when the time of chemical purification increases. Both heat treatment and chemical purification resulted in a decrease in the amount of O_2.

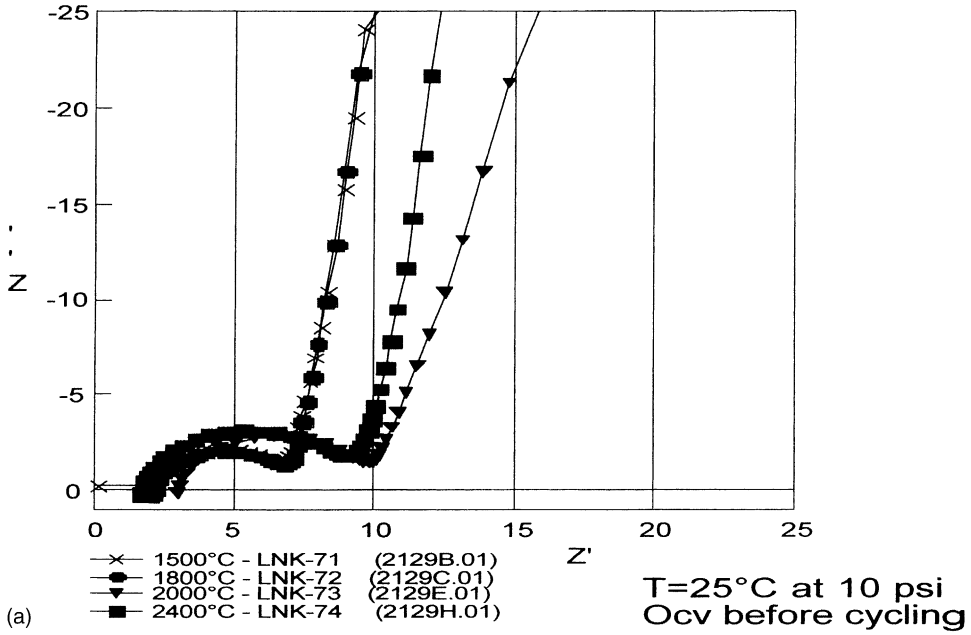

(a)

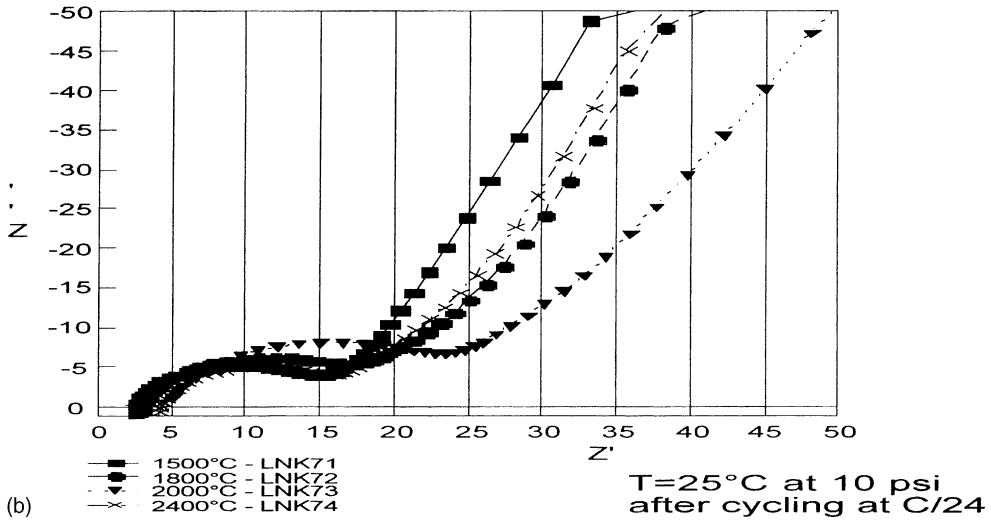

(b)

Fig. 4. Impedance spectra of natural graphite heat-treated at different temperatures: (a) before formation, (b) after formation at 15.5 mA/g (*C*/24 rate).

Table 2
Weight percent of impurities and surface area of graphite after chemical and thermal processes

Element	HQ-42 REF	Thermal purification (wt.%)				Chemical purification (wt.%)		
		HQ-38 1500	HQ-39 C1800	HQ-40 C2000	HQ-41 C2400	HQ-30 C 2 h	HQ-31 C 3 h	HQ-32 C 4 h
Al	0.062	0.19	0.009	<0.001	0.006	0.002	0.018	0.115
Fe	0.144	0.18	0.034	<0.001	<0.001	0.014	0.008	0.004
Si	0.5	0.25	0.14	0.06	0.07	0.24	0.36	0.22
Ca	0.02	0.001	0.001	0.001	0.017	0.006	0.007	0.005
O_2 (%)	1.46	0.18	0.13	0.06	0.05	0.17	0.14	0.18
BET	5.24	4.17	4.36	3.92	4.46	4.394	4.787	4.742

Fig. 1 shows the relation between the irreversible capacity loss (ICL) and reversible capacity versus the degree of purity (chemical process). One can see that the graphite with the highest degree of purity yielded the lowest ICL and highest reversible capacity.

Table 3 summarizes the results [6] obtained by thermal analysis using thermal gravimetric analysis/differential thermal analysis (TGA/DTA) for the oxidation of natural graphite in air before and after milling and by using different chemical processes to purify the sample. The sample obtained by chemical process in $HNO_3 + HF$ produced the highest purity. This sample showed a higher ignition temperature (T_i) than a similar sample obtained by jet mill then followed by chemical purification (i.e. 628 °C versus 568 °C). Unfortunately, the former sample has the highest projected cost. Natural graphite obtained by chemical processing in $H_2SO_4 + XF$ (NH_xF_y) yields the highest ignition temperature. It also exhibited low irreversible capacity loss (91% first-cycle coulombic efficiency) and lowest projected cost.

Fig. 2 shows representative charge–discharge profiles for NG1400 and NG2400 at a discharge rate of 15.5 mA/g (*C*/24 rate). The profiles for these two samples are similar with irreversible voltage plateau at around 800 mV, which is related to decomposition of the electrolyte, and intercalation of lithium in graphite occurring by staging at ∼250 mV to 0 V.

Fig. 3 shows a correlation between the heat-treatment temperature of the natural graphite samples and their electrochemical performances, reversible capacity and first-cycle coulombic efficiency (1EC). The irreversible capacity loss is nearly constant with heat-treatment temperature (HTT) at 1500–2400 °C. The 1EC was 85%, which is lower than that obtained with graphite treated chemically [7] by our process (91% in Table 3). On the other hand, the reversible capacity increases markedly with an increase in HTT.

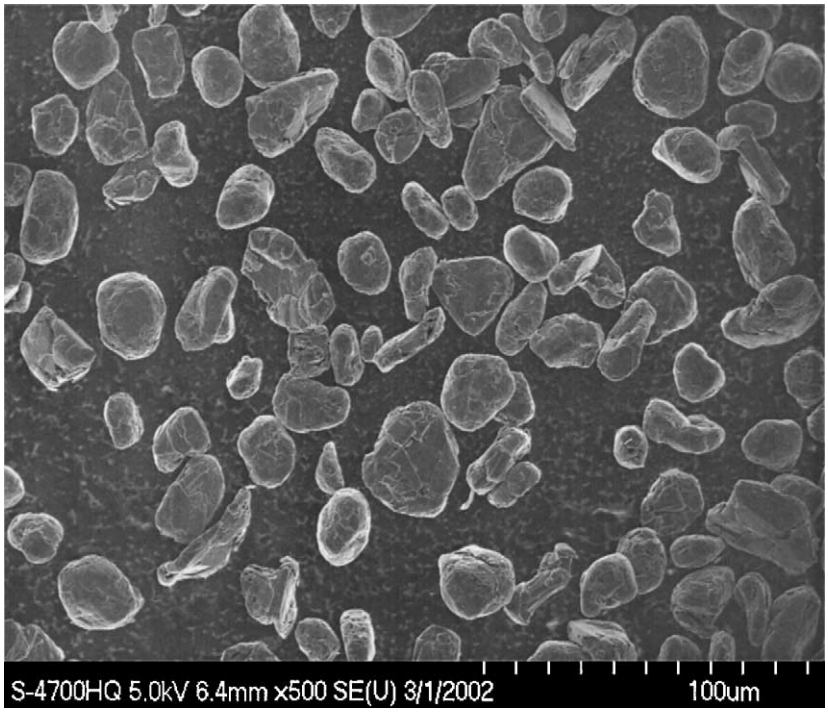

Fig. 5. SEM images of general view of potato-shape natural graphite.

The trend may be related to the decrease in impurity content, but this has not been adequately verified. The constant ICL observed with the heat-treated natural graphites is explainable by analysis of the data obtained by impedance spectroscopy (see Fig. 4). After the formation cycle of the cell at *C*/24 rate, the total impedance ($R_p = R_f + R_C$, R_f is the passivation-film impedance and R_C is the charge-transfer impedance), R_p is almost constant with HTT [8]. This result suggests that the SEI layer formed on heat-treated graphite has similar impedance and consequently the ICL of the samples are comparable.

In our previous work [9], we related the fraction of edge (f_e) and basal plane sites (f_b) for the prismatic structure of natural graphite. The results indicated that $f_e < f_b$, and that Li-ion intercalation in natural graphite occurs mainly at the edge site. To achieve high-rate interaction of Li ions in natural graphite, we must increase the fraction of edge sites which involves modifying the particle morphology from a

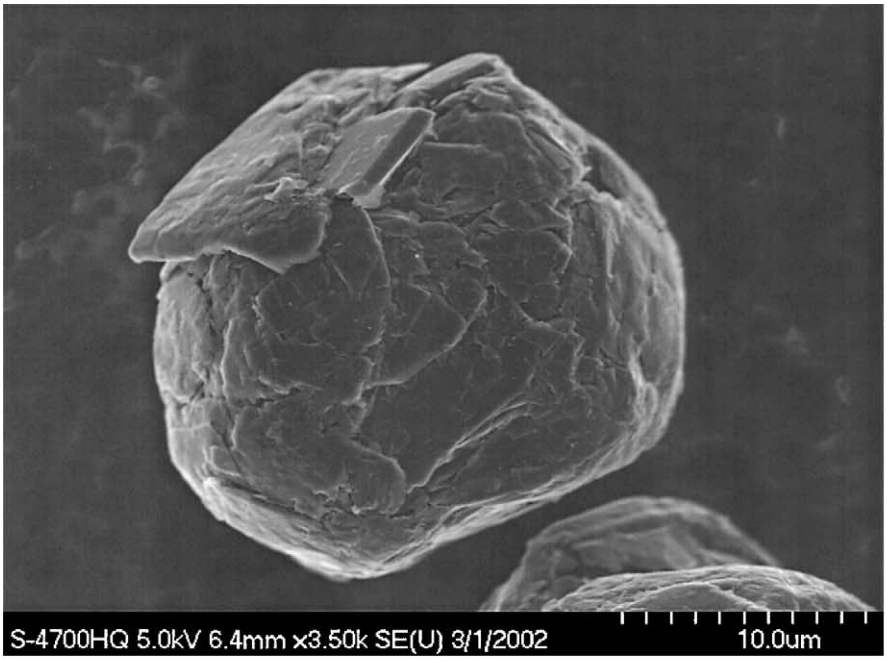

Fig. 6. SEM images of individual potato-shape natural graphite.

Table 3
TGA/DTA summary—oxidation of natural graphite in air

Sample	Treatment	Particle size (μm)	BET area (m^2/g)	Reversible capacity (mAh/g)	First-cycle coulombic efficiency (%)	Ignition temperature (T_i) (°C)
NG-12	–	12	4.34			626
NG-20	–	20	3.2			640
E20 (mill)	No purification	10	6.9	327	79	–
E1 (mill + purification)	HCl + HF	10	6	357	88	633
E2 (mill + purification)	HNO_3+ HF	10	6.6	353	86	628
E3 (mill + purification)	HF	10.5	7.2	365	85	616
E16 (purification + mill)	HCl + HF	12	5.8	362	86	580
E17 (purification + mill)	HNO_3 + HF	12	5.6	397	88	568
E15 (purification + mill)	HF	10	8.7	356	75	570
HQ-16 (mill)	No purification	20	5.4	365	88	608
HQ-24 (mill + purification)	H_2SO_4 + NH_xF_y	20	5.2	361	85	657
HQ-27 (mill + purification)	H_2SO_4 + NH_xF_y	25	3.3	357	91	639

2- to a 3-D structures (referred to as potato shape). We are using two methods to produce the desired graphite particle structure: (i) attrition with metal or ceramic balls, and (ii) modified jet-mill technique [10]. A mathematical model was developed to guide the production of the potato-shape natural graphite.

Fig. 5 shows SEM micrographs of the potato-shape graphite obtained by jet-milling. The particles show only a small variation in shape, which is evident in the different particles shown in Fig. 6a and b. The sphericity of the potato-shape natural graphite is not as regular as that of mesocarbon micro beads (MCMB) because the original natural graphite has a prismatic structure (flake-like).

The composition of intercalation graphite x, in Li_xC_6, that was obtained with natural graphite of different shapes (prismatic and potato shape) is presented in Fig. 7 as a

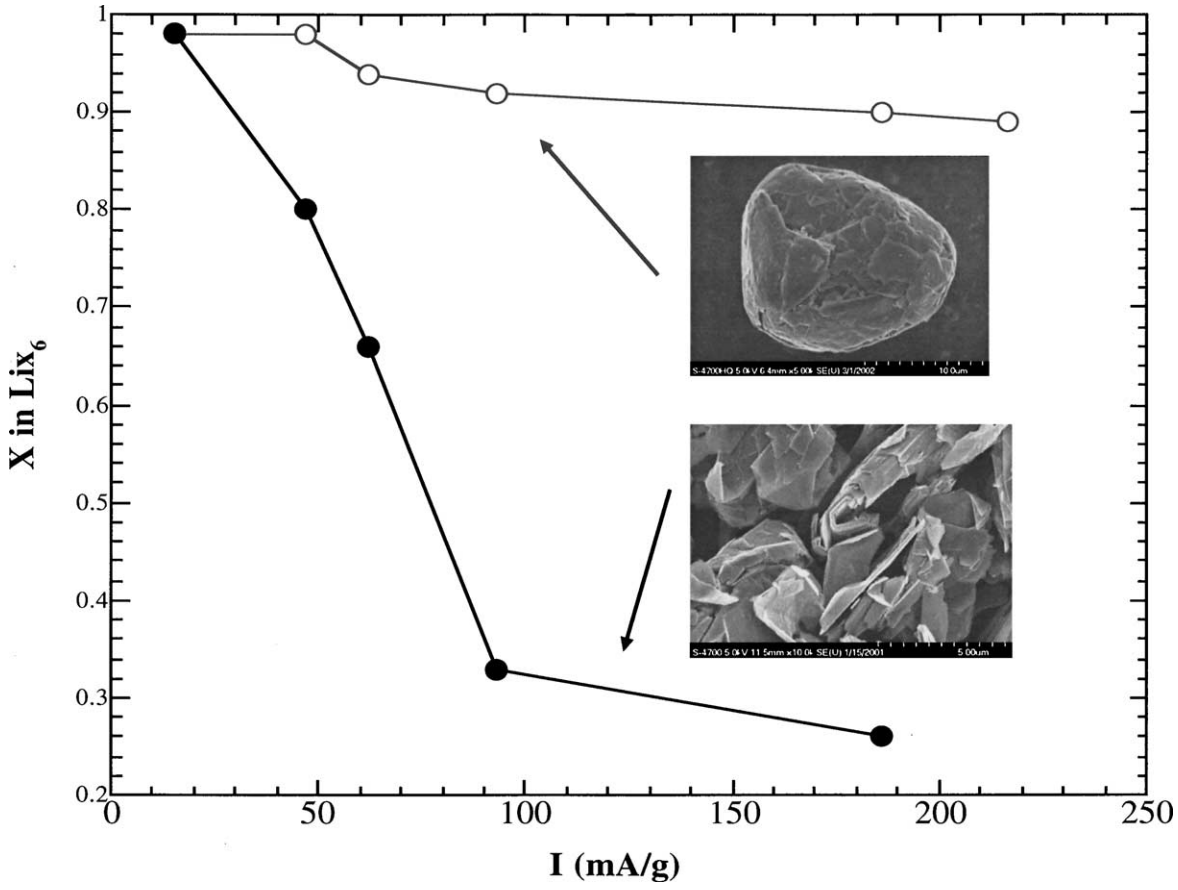

Fig. 7. Composition of intercalated graphites, x in Li_xC_6, vs. current: prismatic vs. potato shape.

function of discharge rate. At low currents, the composition of lithiated graphite approaches the theoretical value, $x = 1$. However, for the prismatic structure, x decreases with an increase in specific current. This trend suggest that solid-state diffusion of Li^+-ion is limiting the intercalation in the flake-like structure. With the potato-shape structure, and at high current, we obtained 90% of the capacity because of the high fraction of edge sites [9]; diffusion of Li^+ ions is rapid with this shape of graphite particles. The potato-shape natural graphite is a very promising material for high-rate capability, because it is easier to fabricate electrodes from this type of graphite. Furthermore, control of the electrode porosity is improved because of the high tap density (i.e. 1.1 cm^3/g) obtained with the potato-shape natural graphite.

4. Concluding remarks

Analysis of the two processes, chemical and thermal, indicate that high reversible capacity is obtained with short chemical treatment time (4 h) or heat treatment at 2400 °C. However, the thermal process of natural graphite to obtain a highly purified sample is costly. The intercalation of Li^+ ions in graphite electrodes in non-aqueous electrolytes involves ion transport in the liquid phase to the edge sites. Our studies indicate that the highest reversible capacity of Li^+ ions at high rate is achieved with 3-D potato-shape graphite, i.e. 90% of the theoretical capacity at *C*-rate.

Acknowledgements

The authors would like to acknowledge the support of Hydro-Quebec and the Assistant Secretary for Energy Efficiency and Renewable Energy, Office of Advanced Automotive Technologies of the U.S. Department of Energy under Contract No. DE-AC03-76SF00098 at Lawrence Berkeley National Laboratory.

References

[1] http://berc.lbl.gov/BATT/BATT.html.
[2] R. Markel et al., US Patent 4,160,813 (1979), Superior Graphite.
[3] T. Takahashi et al., EP 0624913 (1994), Sanyo.
[4] A. Watanabe, JP 57170812A2 (1982), Kyushu Refract Co.
[5] A. Kitahara, JP 3050110A2 (1991), Kansai Coke & Chemical Co.
[6] W. Jiang, G. Nadeau, K. Zaghib, K. Kinoshita, Thermochim. Acta 351 (2000) 85.
[7] K. Zaghib, M. Gauthier, G. Nadeau. A. Guerfi, M. Armand, CA 2299626 (2000), Hydro-Québec.
[8] K. Zaghib, K. Tatsumi, H. Abe, J. Electrochem. Soc. 145 (1998) 210.
[9] K. Zaghib, G. Nadeau, K. Kinoshita, J. Electrochem. Soc. 147 (2000) 2110.
[10] A. Guerfi, F. Brochu, M. Massé, K. Kinoshita, K. Zaghib, CA 2324431 (2000), Hydro-Québec.